



*Citation for published version:*

Suzuki, T, Asami, M & Perry, ACF 2014, 'Asymmetric parental genome engineering by Cas9 during mouse meiotic exit', Scientific Reports, vol. 4, pp. 7621. <https://doi.org/10.1038/srep07621>

*DOI:*

[10.1038/srep07621](https://doi.org/10.1038/srep07621)

*Publication date:*

2014

*Document Version*

Publisher's PDF, also known as Version of record

[Link to publication](#)

*Publisher Rights*

CC BY-NC-ND

This work is licensed under a Creative Commons Attribution-NonCommercial-ShareAlike 4.0 International License. The images or other third party material in this article are included in the article's Creative Commons license, unless indicated otherwise in the credit line; if the material is not included under the Creative Commons license, users will need to obtain permission from the license holder in order to reproduce the material. To view a copy of this license, visit <http://creativecommons.org/licenses/by-nc-sa/4.0/>

## University of Bath

**General rights**

Copyright and moral rights for the publications made accessible in the public portal are retained by the authors and/or other copyright owners and it is a condition of accessing publications that users recognise and abide by the legal requirements associated with these rights.

**Take down policy**

If you believe that this document breaches copyright please contact us providing details, and we will remove access to the work immediately and investigate your claim.



## OPEN

SUBJECT AREAS:  
GENETIC ENGINEERING  
EMBRYOLOGYReceived  
17 October 2014Accepted  
4 December 2014Published  
23 December 2014Correspondence and  
requests for materials  
should be addressed to  
A.C.F.P. (perry135@  
aol.com)\* These authors  
contributed equally to  
this work.Asymmetric parental genome  
engineering by Cas9 during mouse  
meiotic exit

Toru Suzuki\*, Maki Asami\* &amp; Anthony C. F. Perry

Laboratory of Mammalian Molecular Embryology, Department of Biology and Biochemistry, University of Bath, BA2 7AY, England.

Mammalian genomes can be edited by injecting pronuclear embryos with *Cas9* cRNA and guide RNA (gRNA) but it is unknown whether editing can also occur during the onset of embryonic development, prior to pronuclear embryogenesis. We here report *Cas9*-mediated editing during sperm-induced meiotic exit and the initiation of development. Injection of unfertilized, mouse metaphase II (mII) oocytes with *Cas9* cRNA, gRNA and sperm enabled efficient editing of transgenic and native alleles. Pre-loading oocytes with *Cas9* increased sensitivity to gRNA ~100-fold. Paternal allelic editing occurred as an early event: single embryo genome analysis revealed editing within 3 h of sperm injection, coinciding with sperm chromatin decondensation during the gamete-to-embryo transition but prior to pronucleus formation. Maternal alleles underwent editing after the first round of DNA replication, resulting in mosaicism. Asymmetric editing of maternal and paternal alleles suggests a novel strategy for discriminatory targeting of parental genomes.

Gene-targeted mice facilitate functional genetic analysis *in vivo* but the manner in which they are typically produced *via* embryonic stem (ES) cells is laborious, time-consuming and expensive. Gene targeting in larger species, although increasingly relevant in biomedicine, is even more difficult.

Recently, two structurally-discrete classes of DNA binding domain, zinc finger nucleases (ZFNs) and transcription activator-like effector nucleases (TALENs), have been used to generate sequence-specific intracellular double-strand DNA breaks in metazoan genomes. ZFN- or TALEN-generated breaks may be repaired by error-prone nonhomologous end joining (NHEJ) to generate insertions or deletions (indels) that produce non-functional (*null*) alleles in cultured mammalian cells or single-cell embryos<sup>1,2</sup>. ZFN-generated double-strand breaks in cultured cells stimulate high-fidelity homology-dependent repair (HDR) by several orders of magnitude<sup>3–5</sup> and enable HDR-mediated gene targeting in mouse and rat single-cell embryos (known as zygotes) at efficiencies of 2.4–25% (Ref. 1). However, the production of ZFNs and TALENs is complex, and pairs of each must be tailor-made for each targeted region. The efficiency of targeting is also variable and animals have not been produced by simultaneous ZFN- or TALEN-mediated targeting of multiple alleles.

These barriers have recently been negotiated by a powerful newcomer to mammalian genome engineering technology: the clustered, regularly interspaced, short palindromic repeat (CRISPR)/*Cas9* system of adaptable bacterial immunity<sup>6,7</sup>. *Cas9* is a DNA endonuclease whose site-specificity is determined by a single-stranded CRISPR RNA. CRISPR RNAs have been modified from their original bacterial source (*eg Streptococcus pyogenes*) and *Cas9* codon-optimized to function effectively in mammalian cells<sup>6,8</sup>. The *Cas9* system differs from ZFN and TALEN technologies because it utilizes a single protein - *Cas9* - for all modifications, with target specificity provided by modified CRISPR guide RNA (gRNA). The gRNA contains a 20 nucleotide (nt) sequence that forms a heteroduplex with its complementary DNA target (frequently on the genome), which can be any sequence upstream of the proto-spacer adjacent motif (PAM), NGG<sup>6</sup>. Typical gRNAs are relatively short (~110 nt)<sup>6</sup> and thus easy to synthesize. With these advantages, the *Cas9* system has rapidly been adopted to introduce targeted mutations in yeast, plants, *Drosophila*, *C. elegans*, zebrafish, mice, rats, pigs and macaques (reviewed in Ref. 9). *Cas9* has been used for multiplex targeting, with one-step NHEJ-mediated editing of 8 alleles at an efficiency of 10% in human cultured cells and biallelic editing with an 80% hit-rate in single-cell mouse embryos (pronuclear zygotes)<sup>10</sup>. Efficient early embryonic genome targeting is especially promising because it leads directly to mutant offspring<sup>11–14</sup>.

In fertilization, sperm combine with metaphase II (mII) oocytes and become denuded of nucleoprotein (protamine) in a process termed decondensation, before their genomes recondense with maternal histones



and form a nuclear structure, the pronucleus<sup>15–17</sup>. (The maternal genome simultaneously forms a separate pronucleus.) The early phase in which sperm decondensation occurs coincides with the gamete-to-embryo transition and supports efficient transgene integration at quasi-random sites<sup>18,19</sup>; transgenes preferentially integrate into the sperm-derived genome (rather than the oocyte-derived genome), possibly because protein depletion during sperm decondensation makes it a better substrate for recombination<sup>17</sup>. This suggests that the paternal genome might also be a relatively good substrate for Cas9-mediated genome engineering<sup>20</sup>. We sought to test this possibility and report that Cas9 promotes high-efficiency genome editing in the decondensation phase that immediately follows intracytoplasmic sperm injection (ICSI) of unfertilized mII oocytes (Fig. 1A).

## Results and discussion

To evaluate genome editing during meiotic exit, we first generated a test-bed transgenic line (129-eGFP) by introducing a single-copy ubiquitously-expressed *pCAG-eGFP* transgene (*eGFP*) onto the 129/Sv background. When sperm heads from 129-eGFP hemizygotes (*ie eGFP*<sup>+/−</sup> males) were injected into wild-type (wt) B6D2F1 mII oocytes and the resulting embryos cultured, over-all, 90.5% ( $n=116$ ) developed to the blastocyst stage by embryonic day 4 (E4.0), of which 46.6% fluoresced green, indicating that they expressed a functional *eGFP* gene (Fig. 1B,C). When sperm from 129-eGFP hemizygous males were coinjected with 100 ng/μl cRNA encoding Cas9 and 200 ng/μl *eGFP* gRNA (the 1-step method of Fig. 1A), 93.3% developed to the blastocyst stage ( $n=57$ ) but none (0%) fluoresced green (Fig. 1B,C). This is the expected result if the *eGFP* alleles had been efficiently edited to become non-functional.

When we titrated *Cas9* cRNA and *eGFP* gRNA under these conditions, we found that they were effective at concentrations at or above 1–10 ng/μl (Fig. 1C). Paternal mosaicism was occasionally observed at near-threshold concentrations of active gRNA (~1 ng/μl; asterisk in Fig. 1B).

Our previous work has shown that cRNA injected into mII oocytes takes 3–4 h before it is discernibly expressed<sup>21,22</sup>. We therefore reasoned that loading mII oocytes with *Cas9* cRNA prior to sperm/gRNA injection might enhance editing by lengthening the time for *Cas9* expression. To investigate this, we sequentially injected oocytes first with *Cas9* cRNA and after 3–4 h, *eGFP* gRNA plus sperm from a 129-eGFP hemizygote (Fig. 1A). As in the 1-step method, the *Cas9* system efficiently eliminated green fluorescence compared to controls (Fig. 1B–D). These results were confirmed by analogous experiments with a *Nanog-eGFP* knock-in line (Fig. 1E and Supplementary Fig. S1A). This shows that genome targeting by injecting mII oocytes with sperm, *Cas9* cRNA and gRNA can be achieved high efficiencies and is not locus-specific.

To evaluate whether the sequential injection enhanced editing, we performed a comparative titration of gRNA (1-step vs sequential methods), holding the concentration of injected *Cas9* cRNA constant and non-limiting at 100 ng/μl (Fig. 1B–D). Editing in the 1-step method became inefficient when ~1 ng/μl *eGFP* gRNA was injected (Fig. 1C). However, a similar editing efficiency in the sequential method was obtained with 0.01 ng/μl *eGFP* gRNA, corresponding to  $\sim 7 \times 10^8$  gRNA molecules per injection (Fig. 1C). Therefore, in these experiments, the sequential method of *Cas9*-mediated paternal genomic editing was ~100-fold more sensitive than the 1-step method. One interpretation of this finding is that the potential for

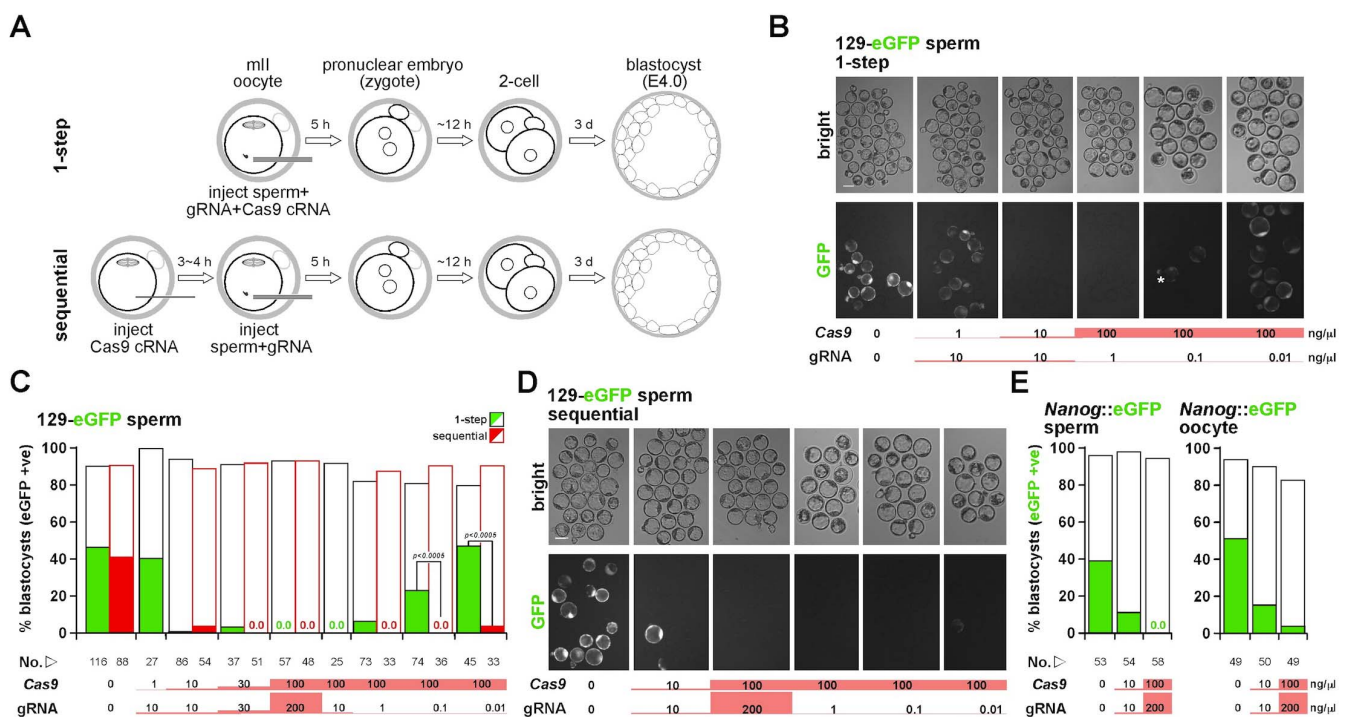


**Figure 1 | Cas9-mediated editing in mII exit following ICSI.** (A) Schematic of 1-step (upper) and sequential methods of Cas9-mediated mII editing. mII, metaphase II. (B) Paired Hoffman modulation (upper) and eGFP expression (eGFP) images of E4.0 blastocysts produced by 1-step injection of wt mII oocytes with 129-eGFP sperm from hemizygotes, with concentrations of injected *Cas9* cRNA and *eGFP* gRNA indicated below. An asterisk indicates a presumptively phenotypic mosaic. Bar, 100 μm. (C) Numerical representation of embryo development and green fluorescence following injection of sperm from 129-eGFP hemizygous males. Percentages are of blastocyst development on embryonic day 4 (E4.0) (open) and of blastocysts that fluoresced green (filled) indicating 129-eGFP transgene expression in 1-step (green) or sequential (red) methods. Starting embryo numbers and injected concentrations of *Cas9* cRNA and *eGFP* gRNA (gRNA) are shown beneath. (D) Paired Hoffman modulation (upper) and eGFP expression (eGFP) images as for (B) except that the sequential method of injection (Fig. 1A) was used. (E) Histograms as for (C) except that one of either the injected sperm (left) or oocyte carried a *Nanog-eGFP* knock-in allele. Red highlights provide at-a-glance indication of RNA concentrations in (B) to (E).



editing in the 1-step method declines before sufficient Cas9 has been synthesized, implying that paternal genome editing is generally an early event.

To assess Cas9 activity towards the maternal genome, wt B6D2F1 sperm were injected into oocytes from females carrying an *eGFP* transgene. Interpretation of these experiments in the 129-*eGFP* line was confounded by carry-over of *eGFP* protein expressed during oocyte maturation, but the problem was mitigated with oocytes from *Nanog-eGFP* hemizygotes, in which there is little or no carry-over (Fig. 1E and Supplementary Fig. S1B). Following injection with 200 ng/μl gRNA and 100 ng/μl *Cas9* cRNA, which targeted the paternal genome with ~100% efficiency, 4.0% of E4.0 blastocysts were GFP-positive ( $49 < n < 58$ ,  $p < 0.0005$ ) (Fig. 1E and Supplementary Fig. S1B).

Direct sequencing of reverse-transcriptase PCR amplicons corresponding to paternal *eGFP* transcripts (*ie* derived from a sperm-borne *eGFP* transgene) in completely non-green-fluorescent E4.0 blastocysts produced unambiguous reads (Fig. 2A,B). The unmixed sequences revealed that single targeting events had occurred to produce indels within or immediately 5' of the gRNA-matching *eGFP* genomic segment ( $n=26$ ) for both sequential and 1-step editing, whether *pCAG-eGFP* or *Nanog-eGFP* transgenes were targeted (Fig. 2A,B). However, targeting of maternal *pCAG-eGFP* or *Nanog-eGFP* transgenes derived from oocytes typically (in 14/15 cases) produced sequence mosaicism (Fig. 2C). In some cases, the sequence ambiguity suggested that cells contained a non-mutated allele as well as a mutated one (Fig. 2C) and *Nanog-eGFP* mutations were detected in two green fluorescent embryos, presumably either reflecting mosaicism or functionality retained by mutated *eGFP* alleles.

These findings suggest that parent-of-origin-specific chromatin behaviour during the gamete-to-embryo transition leads to parental asymmetries in Cas9-mediated genome editing. The generation in most cases of mixed maternal alleles (mosaicism) where only one allele was available for editing indicates that maternal genome editing usually occurred after DNA replication (S-phase). Although maternal editing typically occurred after S-phase, paternal genome editing at non-limiting Cas9 and gRNA concentrations was usually complete pre-S-phase, giving rise to a single event that removed the gRNA target and prevented subsequent editing. Since *pCAG-eGFP* or *Nanog-eGFP* transgenic lines are present in different backgrounds, this phenomenon is allele- and strain-independent.

We next sought to delineate the time-frame for paternal genome editing. To do this, we performed single-cell whole genome amplification and target locus genomic PCR after wt oocytes had been coinjected with *eGFP* transgene-carrying sperm plus Cas9 and gRNA (Fig. 2D). To increase the likelihood of detecting editing in single cells, we used males from a different line carrying 2 *eGFP* transgene copies. Sampling was 3 h after injection. All five (100%) of the transgenic 1-cell embryos analyzed had undergone editing of at least one genomic copy of *eGFP* (Fig. 2D). The 3 h editing time-frame corresponds to the period in which sperm decondensation occurs (Fig. 2E,F), well before pronuclear formation or the onset of mitotic S-phase after ~7 h<sup>23</sup>. This distinguishes Cas9-mediated editing following mII oocyte injection from that following injection of pronuclear zygotes which have entered the mitotic cell cycle and accordingly contain mitotic chromatin<sup>17</sup>.

We next evaluated editing of native alleles in the gamete-to-embryo transition and monitored transmission of mutations to offspring. *Tyr* was chosen because its *null* phenotypes are readily detectable: *Tyr* mutations in C57BL/6 (black) mice result in a white coat colour and/or changes in eye morphology and pigmentation<sup>24,25</sup>. *Cas9* cRNA and *Tyr* gRNA were coinjected with wt C57BL/6 sperm into wt C57BL/6 oocytes and resultant 2-cell embryos transferred to pseudo-pregnant recipient surrogate mothers. Some experiments included an inert gRNA directed against *Foxn1*. Between 14.8 and 24.0% of founders exhibited complete or mosaic phenotypes

expected for loss of *Tyr* function for 1-step and sequential methods (Table 1; Supplementary Fig. S2). These comprised loss of pigmentation in fur and both eyes, sometimes predisposing to ophthalmic irregularities or anophthalmia<sup>26</sup>.

Most (23/27, 85.2%) founder phenotype changes only affected part of the mouse (Supplementary Fig. S2A), reflecting somatic mosaicism and showing that editing had occurred after the first S-phase. We investigated this by sequencing DNA from offspring with and without white coat or eye phenotypes (Supplementary Fig. S3A, B). Most of the founders with evident phenotypic alterations contained one or more *Tyr* mutations (Supplementary Fig. S3A). In addition, many (4/6) randomly-selected founders with no discernable phenotypic changes also possessed *Tyr* mutations. Mutations were typically (10/12) of the mixed type (Supplementary Fig. S3A). Since a similar mixed pattern of mutations was observed for maternal alleles of *eGFP* (Fig. 2C) the phenomenon is not locus- or sequence-specific. Consistent with our findings, multiple edited alleles have also been observed following injection of Cas9/gRNA components into pronuclear zygotes<sup>25</sup>.

Mutations were transmitted to offspring, including inheritance of the non-pigmented eye phenotype in F1 progeny of coat colour founders (with overtly normal eyes), indicating that coat colour and eye phenotypes have a shared aetiology and further revealing founder mosaicism (Supplementary Fig. S2 and Supplementary Fig. S3B).

These experiments demonstrate that injecting mII oocytes with Cas9 cRNA, gRNA and sperm efficiently produces embryos and offspring with edited genomes. Single cell analysis revealed that editing was detectable by 3 h. This period (the first 3 h) overlaps with the gamete-to-embryo transition involving meiotic exit, sperm decondensation (Fig. 2E,F) and polar body cytokinesis<sup>27,28</sup> and precedes by several hours the appearance of pronuclear structures that define the zygote. Recombination within 3 h of sperm delivery would account for the distinctive patterns of paternal and maternal editing we observed (Fig. 2A–C) if sperm decondensation provided a unique genomic opportunity for recombination. Editing of the paternal allele removes the gRNA target, precluding subsequent editing. We did not detect mixed-type paternal allelic editing under optimal, non-limiting conditions (Fig. 1B,C), suggesting that editing occurred during developmental onset, prior to S-phase. By contrast, edited maternal alleles were typically mixed (Fig. 2C). Editing when the Cas9 system is injected into pronuclear zygotes also causes mosaicism<sup>25</sup>, indicating that the same mechanism operated. This implies that, consistent with observations in transgenesis<sup>18</sup>, meiotic exit and the gamete-to-embryo transition do not efficiently support maternal genome editing, plausibly because the structure of maternal chromatin during this phase is refractory to the editing machinery. Although the maternal genome is inherently refractory to editing in the gamete-to-embryo transition, the limited evidence here for paternal genome editing in zygotes presumably reflects the removal of available targets by efficient editing at the earlier stage (Fig. 2F).

Genome editing during meiotic progression has several practical implications. The possibility that the paternal genome is preferentially targeted during decondensation implies that it might be possible to devise strategies to alter only one parental allele prescriptively, even where both have identical DNA sequences. Selective editing of the paternal allele, for example, may have utility in the study of imprinting or to alter subtle deleterious (epi)mutations. The relative recombinogenicity of decondensing paternal chromatin also opens the possibility that it might support a broader repertoire of targeting strategies, including the use of 'nickases' (Ref. 28), nuclear transfer, different delivery platforms<sup>29</sup>, and the efficient deletion<sup>12</sup> or integration<sup>30</sup> of large DNA fragments; a comprehensive evaluation of large fragment targeting would benefit from a more complete description of HDR in mammalian mII oocytes<sup>20</sup>.



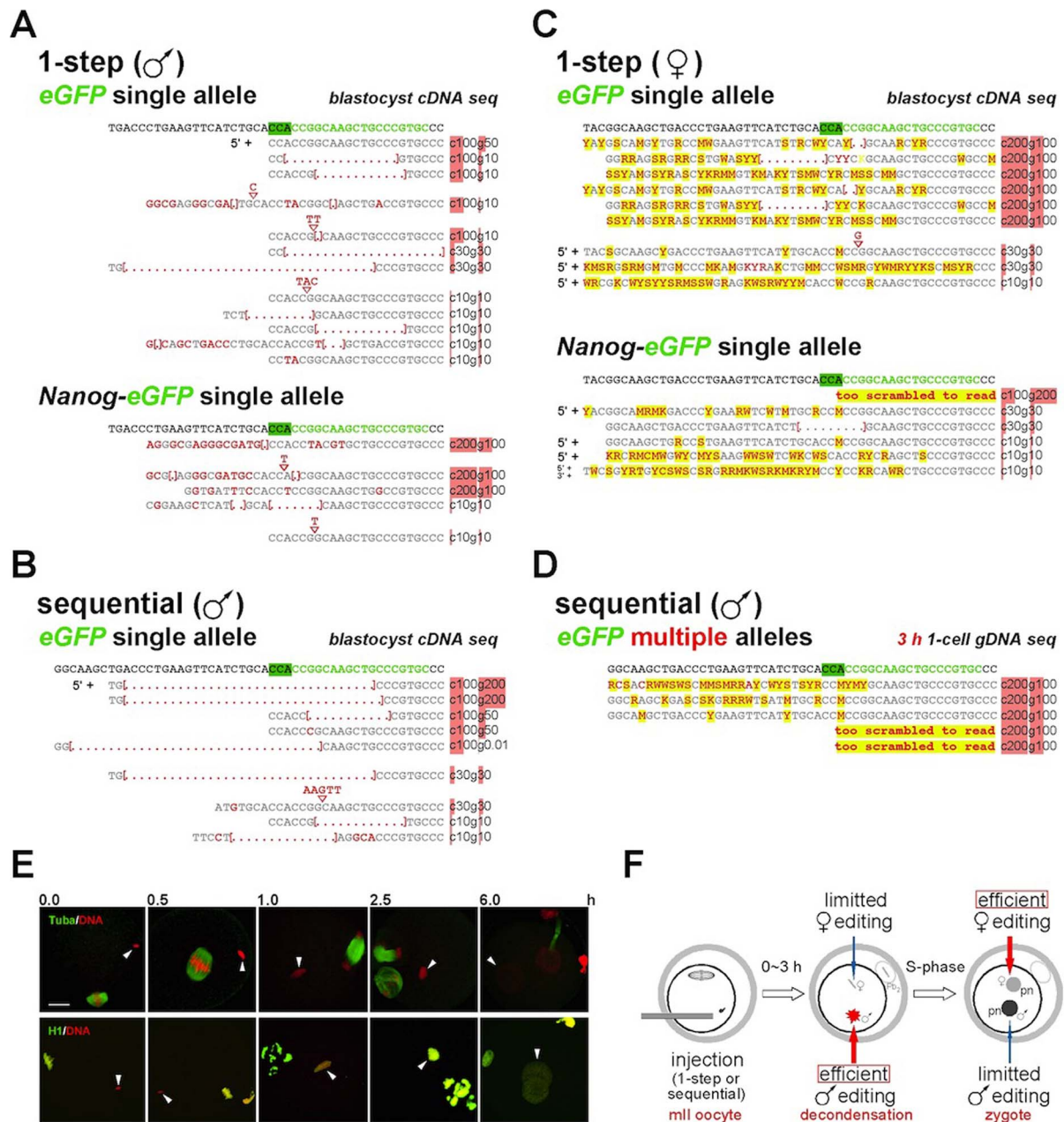


**Figure 2 | Sequence analysis reveals allelic asymmetry in parental genome mII editing.** (A) Sequences of reverse-transcriptase PCR products from embryonic day 4 (E4.0) blastocysts developing after the 1-step method of editing (Fig. 1A) in which *Cas9* cRNA and *eGFP* gRNA were co-injected into mII oocytes with sperm from 129-*eGFP* single-copy hemizygotes (*eGFP* single). The gRNA-target sequence (green typeface) plus adjacent 5' sequence is displayed on the top row and mutants beneath (grey typeface), with the corresponding *Cas9* cRNA (c) and *eGFP* gRNA (g) concentrations (ng/μl) that were injected to produce them. The proto-spacer adjacent motif (PAM) is highlighted in green. Mutations are indicated in red typeface. 5' +, mutations detected 5' (but not 3') of the displayed sequence. (B) Sequences of editing mutants produced as per (A), by injecting sperm from 129-*eGFP* (upper) or *Nanog-eGFP* knock-in hemizygotes with wt oocytes, except by the sequential method (Fig. 1A). (C) Sequences of editing mutants as for (A), except that the transgenic alleles were maternal; wt 129 sperm were injected into mII oocytes obtained from 129-*eGFP* single copy (upper) or *Nanog-eGFP* knock-in hemizygotes. 3' +, mutations were detected 3' of the displayed sequence. Yellow highlighting indicates ambiguous calls presumably produced by multiple targeting events. (D) Whole genome amplification of individual embryos collected 3 h after injection with sperm from a hemizygous transgenic line (*eGFP* multi) carrying two copies of the *eGFP* transgene. The annotation used is as for (C). Red highlights provide at-a-glance indication of RNA concentrations in (A) to (D). (E) Merged confocal immunofluorescence images of single embryos at the times indicated (h) after ICSI, showing DNA labelled with propidium iodide (red) and antibody labeling (green) of tubulin-α (Tuba, upper panels) or histone H1 (H1). Both sperm and oocytes were wt. White arrowheads indicate paternal chromatin. Bar, 100 μm. (F) Schematic depicting a model for *Cas9*-mediated editing following injection of mII oocytes (mII). Limited editing of maternal alleles during the gamete-to-embryo transition is inherent to the system, whereas limited editing of paternal alleles in zygotes is because available targets have already been removed. Pb<sub>2</sub>, second polar body; pn, pronucleus.

In addition, editing during the gamete-to-embryo transition may have utility in larger species. Although obtaining pronuclear zygotes is relatively straightforward in the mouse, this is not always the case

for large commercial breeds and the efficiency of integration and transmission of exogenous DNA remains low<sup>31</sup>. The use of mII oocytes, which in some species (eg pigs) can be derived by *in vitro*

Table 1 | Development of embryos and phenotypes of offspring in experiments to edit *Tyr* alleles

method	[gRNA]	[Cas9 cRNA]	in vitro				in vivo				
			survived	pn	2-cell	blast	born/ff	preg/ff	white	mosaic	% phen
1-step	Tyr30	30 ng/μl	148/160	136	132	19/26	60/106	7/7	0	9	15.8
1-step	Tyr30 + Fox30	30 ng/μl	129/148	128	127	17/25	11/60	1/3	0	2	20.0
1-step	Tyr 200	100 ng/μl	59/67	57	56	7/8	28/48	3/3	2	4	24.0
1-step	Tyr200 + Fox200	100 ng/μl	54/67	51	48	nd	31/48	3/3	0	5	17.9
seq	Tyr30 + Fox30	30 ng/μl	84/93	78	78	8/18	30/60	3/3	2	2	14.8

Experiments were initiated on  $\geq 2$  experimental days for each treatment. seq, sequential method (Fig. 1A); Tyr30, Tyr gRNA at 30 ng/μl; Fox30, Foxn1 gRNA at 30 ng/μl; pn, pronuclear embryos 6–8 h after sperm injection; blast, blastocyst; nd, not determined; ff, embryo transfer at the 2-cell stage; preg, number of recipients (recipients falling pregnant). Mosaic phenotypes group coat colour and eye changes. Some pups were rejected by foster mothers prior to weaning. Percentages with phenotype changes (% phen) exclude pups that died perinatally.

maturation, may address this limitation, with delivery of the editing system by ICSI<sup>32</sup> or other methods<sup>29</sup>. Finally, ICSI in human assisted reproduction is widely used<sup>33</sup> and this or analogous approaches may one day enable human genome targeting or editing during very early development. This formal possibility will require exhaustive evaluation, but if successful, could enable genomic surgery for gene repair during the initiation of embryogenesis.

## Methods

**Animals.** Animal procedures complied with the statutes of the Animals (Scientific Procedures) Act, 1986, approved by the University of Bath Animal Welfare and Ethical Review Body and the Biosciences Services Unit. Wild-type mouse strains were bred from stocks in-house or otherwise supplied by Charles River (L'Arbresle, France). A *pCAG-eGFP* transgene was introduced into the 129Sv background to produce multi- and single-copy, high-expressing lines<sup>18</sup>, and additional transgenic lines were generated in-house or were kind gifts and contained *pCAG-eGFP* or *pNanog-eGFP* transgenes on mixed background hybrid lines containing a contribution from C57BL/6.

**Collection and culture of oocytes.** Oocytes were collected from 8–12-week-old females following standard super-ovulation by serial intraperitoneal injection of 5 IU pregnant mare serum gonadotropin (PMSG) and 5 IU human chorionic gonadotropin (hCG). Oviductal metaphase II (mII) oocytes were collected in M2 medium (Specialty Media, USA) ~15 h post-hCG injection essentially as described<sup>34</sup>. After repeated washing in M2, denuded oocytes were incubated in kalium simplex optimized medium (KSOM; Specialty Media, USA)<sup>35</sup> under mineral oil in humidified 5% CO<sub>2</sub> (v/v air) at 37°C, until required.

**Sperm preparation and microinjection.** Sperm preparation was essentially as previously described<sup>21,22</sup>. Briefly, cauda epididymal sperm from 8–12-week-old males were triturated for 45 sec in nuclear isolation medium (NIM; 125 mM KCl, 2.6 mM NaCl, 7.8 mM Na<sub>2</sub>HPO<sub>4</sub>, 1.4 mM KH<sub>2</sub>PO<sub>4</sub>, 3.0 mM EDTA; pH 7.0) containing 1.0% (w/v) 3-[(3-cholamidopropyl)dimethylammonio]-1-propanesulfonate (CHAPS) at room temperature (25°C). Sperm were washed twice in NIM and pelleted (1,890 g) at ambient temperature; head-tail detachment was enhanced by trituration during pellet resuspension. Sperm were resuspended in ice-cold NIM (~0.5 ml per epididymis) and stored at 4°C for up to 3 h until injection. Typically, ~50 μl of each suspension was mixed with 20 μl of polyvinylpyrrolidone (PVP, average *M<sub>n</sub>* ≈ 360,000; Sigma, UK) solution (15% (w/v)) and sperm injected (ICSI) using a piezo-actuated pipette (Prime Tech, Japan) into oocytes in a droplet of M2 within ~60 min, essentially as described<sup>34</sup>. Assuming an inner pipette tip diameter of 6 μm, we estimate that 2–2.5 pl were introduced per injection. After a brief (5–15 min) recovery period, injected oocytes were transferred to KSOM under mineral oil equilibrated in humidified 5% CO<sub>2</sub> (v/v air) at 37°C.

**Immunocytochemistry and imaging.** Immunocytochemistry, differential interference contrast microscopy (DIC) and fluorescence imaging were essentially as described previously<sup>21,22</sup>. In brief, mII oocyte and 1-cell embryo samples for the images in Figure 2E were incubated overnight at 4°C with mouse anti-α-tubulin (1:2000 [v/v]; Sigma) or -H1 (1:1000; Santa Cruz, USA) antibodies, followed by a 1 h incubation at 37°C with secondary antibody (1:250; Life Technologies Ltd., UK) conjugated to Alexa 488. DNA was stained by incubating samples at 37°C for 20 min in propidium iodide (1:200; Sigma, USA). Fluorescence was visualized on an Eclipse E600 (Nikon, Japan) microscope equipped with a Radiance 2100 laser scanning confocal system (BioRad, USA). Images were processed with ImageJ (<http://imagej.nih.gov/ij/>) analysis software. Embryos were imaged on an Olympus IX71 equipped with an Andro Zyla sCMOS camera and OptoLED illumination system (Cairn Research Ltd., UK) and processed using Metamorph software (Molecular Devices, LLC, USA). Excitation at 484 nm with an ET-EYFP filter system was used to detect eGFP epifluorescence. Imaging of blastocysts for Figure 1 and Supplementary Figure S1 was following culture in drops of KSOM (Specialty Media, USA) under mineral oil in 6 cm dishes in a humidified 5% CO<sub>2</sub> (v/v air) incubator at 37°C<sup>21,22</sup>.

**Embryo transfer.** E1.5 (2-cell) embryos (the day following activation) were transferred to the oviductal ampullae of pseudo-pregnant CD-1 females at day 0.5 (ie plugged females that had been mated with vasectomized males the previous night). Pups were delivered by natural birth and where appropriate, fetuses, pups and placentae collected by Caesarian section at the desired time point. Newborn pups were fostered by CD-1 females as appropriate.

**Vector construction.** For target gRNA synthesis, we employed the pT7-gRNA backbone vector system<sup>36</sup>. Target gRNA sequences were selected using the CRISPR gRNA design tool (DNA 2.0) and informed the design of complementary oligonucleotides of the general sequences: TAGGN<sub>20</sub> (forward) and AAACN<sub>20</sub> (reverse) (Eurofins MWG Operon). Forward and reverse oligonucleotides (10 μM each) were annealed by incubating in 20 μl 1× NEB buffer solution at 95°C for 5 min, ramping down to 50°C at 0.1°C/sec followed by 50°C for 10 min then ramping to 4°C at 1°C/sec. 1 μl of annealed oligonucleotides were mixed with 400 ng of pT7-gRNA vector, 0.5 μl *Bsm*BI, 0.3 μl *Bgl*II, 0.3 μl *Sal*GI, 0.5 μl T4 DNA ligase, 1 μl 10× NEB buffer 3, 1 μl T4 ligase buffer and 4 μl nuclease-free water. One-step digestion and ligation were performed in a PCR machine using the parameters: 3 cycles of 37°C for 20 min, 16°C for 15 min, followed by incubation at 37°C for 10 min and 55°C for 15 min. Products (2 μl) were used to transform DH5α. Positives (>90%) were verified by diagnostic *Bgl*II digestion and sequencing and purified pT7-gRNA constructs were linearized by *Bam*HI digestion and used to program *in vitro* gRNA synthesis using a MEGAscript T7 Transcription Kit (Life Technologies).

**Synthesis of cRNA and gRNA.** 5'-capped and polyadenylated Cas9 cRNA was synthesized in a T7 mScript™ Standard mRNA Production System (Cellscript, USA) as previously described<sup>21,22</sup> from the T7 P3s-Cas9HC vector. Guide RNA (gRNA) was synthesized using a MEGAscript T7 Transcription Kit (Invitrogen, USA) according to the instructions of the manufacturer. RNAs were dissolved in nuclease-free water, quantified on a nanophotometer (Implen, Germany) and stored in aliquots at -80°C until required. Immediately prior to injection, RNA solutions were diluted as appropriate with nuclease-free water. In the sequential injection method, oocytes were first injected with Cas9 cRNA solution and following culture for 3–4 h the same oocyte was injected with a single sperm in the appropriate gRNA dilution. For 1-step injection, gRNA and Cas9 cRNA were mixed with a sperm suspension to give the appropriate final injection concentrations and a single sperm injected into the oocyte. Following injection, embryos were cultured *in vitro* either to the blastocyst stage to allow evaluation of genome editing in preimplantation embryos, or transferred at the 2-cell stage to pseudopregnant recipients so that mutations could be characterised in offspring.

**Genomic DNA analysis.** For standard genotyping, mouse ear-punch tissue samples were digested at 55°C for 3 h in 25–100 μl of a lysis buffer containing 10% (w/v) sodium dodecyl sulphate and with 2 mg/ml proteinase K (Sigma). 1 μl of a 1:10 dilution of each sample was used for genotyping by PCR in a 20 μl reaction volume.

For genomic qPCR, crude lysates were diluted 50-fold and 5 μl mixed with 20 μl SYBR® Green PCR Master Mix (Life Technologies). qPCR was performed on an ABI7500 Real Time PCR machine (Applied Biosystems) with the following parameters: 95°C, 10 sec (once); 95°C, 5 sec; 62°C, 31 sec (40 cycles); 72°C, 35 sec (once). DNA from the *Nanog-eGFP* line served as a single eGFP copy reference. Relative expression of eGFP was calculated using the  $\Delta\Delta C_t$  between eGFP and *H3f3a*. Fold change was calculated as  $E = 2^{-\Delta\Delta C_t}$ . Sequences of PCR primers used here are given in Supplementary Table S1.

Whole genome amplification of single oocytes 3 h post-ICSI was performed with a GenomePlex® Single Cell Whole Genome Amplification kit (Sigma) in accordance with the supplied instructions. In brief, mII oocytes from superovulated B6D2F1 females were injected with sperm from either 129-GFP homozygous or hemizygous 8–12-week-old males. Injected cells were singly transferred to a 0.2 ml PCR tube in a minimal volume 3 h after ICSI and flash-frozen until processing shortly after. Frozen samples were adjusted to 9 μl with nuclease-free water and single-cell lysis and DNA fragmentation were performed by heating to 50°C for 1 h followed by 99°C for 4 min in the presence of 1 μl Proteinase K (0.5 mg/ml) in the Single Cell Lysis & Fragmentation Buffer provided. Library preparation was performed on fragmented DNA samples using the solution provided and incubated in a thermal cycler with the



following parameters (one cycle): 16°C, 20 min; 24°C, 20 min; 37°C, 20 min; 75°C, 5 min; hold at 4°C. Genome amplification was performed with the addition of 7.5 µl Amplification Master Mix and 5.0 µl WGA DNA polymerase in a thermal cycler with the following parameters immediately after a single denaturing step (95°C, 3 min): 94°C, 30 sec; 65°C, 5 min (25 cycles); hold at 4°C. Using WGA samples as input DNA, *eGFP* sequences were amplified by PCR (Supplementary Table S1) and amplicons purified from 1.4% (w/v) agarose gels using the Wizard® SV Gel and PCR Clean-Up System (Promega) and supplied for sequencing with mixed read sequences (Source BioScience).

**Statistical analysis.** Statistical differences between pairs of data sets were analyzed by a chi-squared test.

1. Cui, X. *et al.* Targeted integration in rat and mouse embryos with zinc-finger nucleases. *Nat. Biotechnol.* **29**, 64–67 (2011).
2. Sung, Y. *et al.* Knockout mice created by TALEN-mediated gene targeting. *Nat. Biotechnol.* **31**, 23–24 (2013).
3. Porteus, M. H. & Baltimore, D. Chimeric nucleases stimulate gene targeting in human cells. *Science* **300**, 763 (2003).
4. Urnov, F. D. *et al.* Highly efficient endogenous human gene correction using designed zinc-finger nucleases. *Nature* **435**, 646–651 (2005).
5. Meyer, M., de Angelis, M. H., Wurst, W. & Kühn, R. (2010). Gene targeting by homologous recombination in mouse zygotes mediated by zinc-finger nucleases. *Proc. Natl. Acad. Sci. USA* **107**, 15022–15026.
6. Mali, P. *et al.* RNA-guided human genome engineering via Cas9. *Science* **339**, 823–826 (2013).
7. Hsu, P. D., Lander, E. S. & Zhang, F. Development and applications of CRISPR-Cas9 for genome engineering. *Cell* **157**, 1262–1278 (2014).
8. Cong, L. *et al.* Multiplex genome engineering using CRISPR/Cas systems. *Science* **339**, 819–823 (2013).
9. Sander, J. D. & Joung, J. K. CRISPR-Cas systems for editing, regulating and targeting genomes. *Nat. Biotechnol.* **32**, 347–355 (2014).
10. Wang, H. *et al.* One-step generation of mice carrying mutations in multiple genes by CRISPR/Cas-mediated genome engineering. *Cell* **153**, 910–918 (2013).
11. Shen, B. *et al.* Generation of gene-modified mice via Cas9/RNA-mediated gene targeting. *Cell Res.* **23**, 720–723 (2013).
12. Fujii, W., Kawasaki, K., Sugiura, K. & Naito, K. Efficient generation of large-scale genome-modified mice using gRNA and CAS9 endonuclease. *Nucleic Acids Res.* **41**, e187 (2013).
13. Yang, H. *et al.* One-step generation of mice carrying reporter and conditional alleles by CRISPR/Cas-mediated genome engineering. *Cell* **154**, 1370–1379 (2013).
14. Zhou, J. *et al.* One-step generation of different immunodeficient mice with multiple gene modifications by CRISPR/Cas9 mediated genome engineering. *Int. J. Biochem. Cell Biol.* **46**, 49–55 (2014).
15. Yanagimachi, R. Mammalian fertilization. In: *The Physiology of Reproduction* (E. Knobil & J. D. Neill, eds), 2nd edition, pp. 189–317. Raven Press, New York (1994).
16. McLay, D. W. & Clarke, H. J. Remodelling the paternal chromatin at fertilization in mammals. *Reproduction* **125**, 625–633 (2003).
17. Yoshida, N., Brahmajosyula, M., Shoji, S., Amanai, M. & Perry, A. C. F. Epigenetic discrimination by mouse metaphase II oocytes mediates asymmetric chromatin remodeling independently of meiotic exit. *Dev. Biol.* **301**, 464–477 (2007).
18. Perry, A. C. F. *et al.* Mammalian transgenesis by intracytoplasmic sperm injection. *Science* **284**, 1180–1183 (1999).
19. Perry, A. C. F. *et al.* Efficient metaphase II transgenesis with different transgene archetypes. *Nature Biotechnol.* **19**, 1071–1073 (2001).
20. Perry, A. C. F. Hijacking oocyte DNA repair machinery in transgenesis? *Mol. Reprod. Dev.* **56**, 319–324 (2000).
21. Suzuki, T., Yoshida, N., Suzuki, E., Okuda, E. & Perry, A. C. F. Full-term mouse development by abolishing Zn<sup>2+</sup>-dependent metaphase II arrest without Ca<sup>2+</sup> release. *Development* **137**, 2659–2669 (2010).
22. Suzuki, T. *et al.* Mouse Emi2 as a distinctive regulatory hub in second meiotic metaphase. *Development* **137**, 3281–3291 (2010).
23. Aoki, F. & Schultz, R. M. DNA replication in the 1-cell mouse embryo: stimulatory effect of histone acetylation. *Zygote* **7**, 165–172 (1999).
24. Mizuno, S. *et al.* Simple generation of albino C57BL/6J mice with G291T mutation in the tyrosinase gene by the CRISPR/Cas9 system. *Mamm. Genome* **25**, 327–334 (2014).
25. Yen, S. T. *et al.* Somatic mosaicism and allele complexity induced by CRISPR/Cas9 RNA injections in mouse zygotes. *Dev. Biol.* **393**, 3–9 (2014).
26. Cronin, C. A., Ryan, A. B., Talley, E. M. & Scrable, H. Tyrosinase expression during neuroblast divisions affects later pathfinding by retinal ganglion cells. *J. Neurosci.* **23**, 11692–11697 (2003).
27. Perry, A. C. F. & Verlhac, M.-H. Second meiotic arrest and exit in frogs and mice. *EMBO Rep.* **9**, 246–251 (2008).
28. Mali, P. *et al.* CAS9 transcriptional activators for target specificity screening and paired nickases for cooperative genome engineering. *Nat. Biotechnol.* **31**, 833–838 (2013).
29. Lois, C., Hong, E. J., Pease, S., Brown, E. J. & Baltimore, D. Germline transmission and tissue-specific expression of transgenes delivered by lentiviral vectors. *Science* **295**, 868–872 (2002).
30. Gennequin, B., Otte, D. M. & Zimmer, A. CRISPR/Cas-induced double-strand breaks boost the frequency of gene replacements for humanizing the mouse *Cnr2* gene. *Biochem. Biophys. Res. Commun.* **441**, 815–819 (2013).
31. Robl, J. M., Wang, Z., Kasinathan, P. & Kuroiwa, Y. Transgenic animal production and animal biotechnology. *Theriogenology* **67**, 127–133 (2007).
32. Onishi, A. & Perry, A. C. F. “Livestock Production via Micromanipulation” pp 371–375 in ‘Practical Manual of In Vitro Fertilization’. Nagy, Z. P., Varghese, A. C. and Agarwal, A. (Eds.) Springer, US (2012).
33. Mansour, R. *et al.* International Committee for Monitoring Assisted Reproductive Technologies world report: Assisted Reproductive Technology 2006. *Hum. Reprod.* **29**, 1536–1551 (2014).
34. Yoshida, N. & Perry, A. C. F. Piezo-actuated mouse intracytoplasmic sperm injection (ICSI). *Nature Protoc.* **2**, 296–304 (2007).
35. Erbach, G. T., Lawitts, J. A., Papaioannou, V. E. & Biggers, J. D. Differential growth of the mouse preimplantation embryo in chemically defined media. *Biol. Reprod.* **50**, 1027–1033 (1994).
36. Jao, L. E., Wente, S. R. & Chen, W. Efficient multiplex biallelic zebrafish genome editing using a CRISPR nuclease system. *Proc. Natl. Acad. Sci. USA* **110**, 13904–13909 (2013).

## Acknowledgments

The authors thank Animal Facility support staff for ensuring the welfare of animals used in this work. We are grateful to Drs M. Leeb, M. VerMilyea, M. Furutani-Seiki, J. Correia and Mr D. Sharma and acknowledge Project Grant support from the Medical Research Council, UK (G1000839) and an EU Reintegration Grant (PIRG06-GA-2009-256408) to A.C.F.P.

## Author contributions

A.C.F.P. conceived the experiments with additional input from T.S. and M.A. Micromanipulation was performed by T.S. and molecular analyses by M.A. Data analysis was by T.S., M.A. and A.C.F.P. A.C.F.P. wrote the manuscript with suggestions from T.S. and M.A.

## Additional information

**Supplementary information** accompanies this paper at <http://www.nature.com/scientificreports>

**Competing financial interests:** The authors declare no competing financial interests.

**How to cite this article:** Suzuki, T., Asami, M. & Perry, A. C. F. Asymmetric parental genome engineering by Cas9 during mouse meiotic exit. *Sci. Rep.* **4**, 7621; DOI:10.1038/srep07621 (2014).



This work is licensed under a Creative Commons Attribution-NonCommercial-ShareAlike 4.0 International License. The images or other third party material in this article are included in the article's Creative Commons license, unless indicated otherwise in the credit line; if the material is not included under the Creative Commons license, users will need to obtain permission from the license holder in order to reproduce the material. To view a copy of this license, visit <http://creativecommons.org/licenses/by-nc-sa/4.0/>